



Excitonic luminescence of hemiporphyrazines

Huber, Sabrina M ; Seyfried, Martin S ; Linden, Anthony ; Luedtke, Nathan W

Abstract: Metal-free hemiporphyrazine (HpH2) is a notoriously insoluble material possessing interesting photophysical properties. Here we report the synthesis, structure, and photophysical properties of an octahedral zinc trans-ditriflate hemiporphyrazine complex “HpH2Zn(OTf)2” that contains a neutral hemiporphyrazine ligand. The photophysical properties of hemiporphyrazine are largely unaffected by introduction of zinc(II) triflate, but a dramatic increase in solubility is observed. HpH2Zn(OTf)2 therefore provides a convenient model system to evaluate the impact of aggregation on the photophysical properties of hemiporphyrazine. Soluble aggregates and crystalline materials containing planar hemiporphyrazines exhibit relatively strong absorbance of visible light (450–600 nm) and red luminescence (600–700 nm). Hemiporphyrazine monohydrate (HpH2 · H2O), in contrast, has a nonplanar “saddle-shaped” conformation that exhibits very little absorbance of visible light in solution or in the solid state. Upon photoexcitation at 380 nm, HpH2Zn(OTf)2 and HpH2 exhibit multiwavelength emissions centered at 450 and 650 nm. Emissions at 450 nm are highly anisotropic, while emissions at 650 nm are fully depolarized with respect to a plane-polarized excitation source. Taken together, our results suggest that excitonic coupling of aggregated and crystalline hemiporphyrazines results in increased absorbance and emission of visible light from S0 → S1 transitions that are usually symmetry forbidden in isolated species. In contrast to previously proposed theories involving excited-state intramolecular proton transfer, we propose that the multiple-wavelength luminescent emissions of HpH2Zn(OTf)2 and HpH2 are due to emissive S1 and S2 states in aggregated and crystalline hemiporphyrazines. These results may provide a better understanding of the nonlinear optical properties of these materials in solution and in the solid state.

DOI: <https://doi.org/10.1021/ic2017566>

Posted at the Zurich Open Repository and Archive, University of Zurich

ZORA URL: <https://doi.org/10.5167/uzh-71528>

Journal Article

Accepted Version

Originally published at:

Huber, Sabrina M; Seyfried, Martin S; Linden, Anthony; Luedtke, Nathan W (2012). Excitonic luminescence of hemiporphyrazines. *Inorganic chemistry*, 51(13):7032-7038.

DOI: <https://doi.org/10.1021/ic2017566>

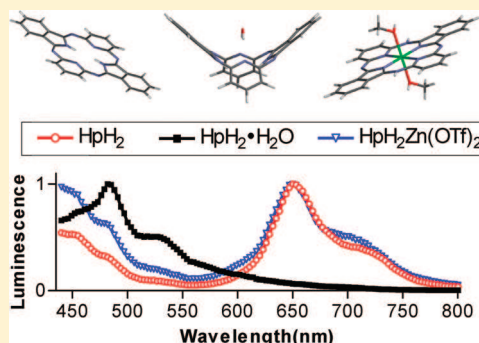
Excitonic Luminescence of Hemiporphyrazines

Sabrina M. Huber, Martin S. Seyfried, Anthony Linden, and Nathan W. Luedtke*

Institute of Organic Chemistry, University of Zürich, Winterthurerstrasse 190, Switzerland, 8057

S Supporting Information

ABSTRACT: Metal-free hemiporphyrazine (HpH₂) is a notoriously insoluble material possessing interesting photophysical properties. Here we report the synthesis, structure, and photophysical properties of an octahedral zinc trans-ditriflate hemiporphyrazine complex “HpH₂Zn(OTf)₂” that contains a neutral hemiporphyrazine ligand. The photophysical properties of hemiporphyrazine are largely unaffected by introduction of zinc(II) triflate, but a dramatic increase in solubility is observed. HpH₂Zn(OTf)₂ therefore provides a convenient model system to evaluate the impact of aggregation on the photophysical properties of hemiporphyrazine. Soluble aggregates and crystalline materials containing planar hemiporphyrazines exhibit relatively strong absorbance of visible light (450–600 nm) and red luminescence (600–700 nm). Hemiporphyrazine monohydrate (HpH₂·H₂O), in contrast, has a nonplanar “saddle-shaped” conformation that exhibits very little absorbance of visible light in solution or in the solid state. Upon photoexcitation at 380 nm, HpH₂Zn(OTf)₂ and HpH₂ exhibit multiwavelength emissions centered at 450 and 650 nm. Emissions at 450 nm are highly anisotropic, while emissions at 650 nm are fully depolarized with respect to a plane-polarized excitation source. Taken together, our results suggest that excitonic coupling of aggregated and crystalline hemiporphyrazines results in increased absorbance and emission of visible light from S₀ ↔ S₁ transitions that are usually symmetry forbidden in isolated species. In contrast to previously proposed theories involving excited-state intramolecular proton transfer, we propose that the multiple-wavelength luminescent emissions of HpH₂Zn(OTf)₂ and HpH₂ are due to emissive S₁ and S₂ states in aggregated and crystalline hemiporphyrazines. These results may provide a better understanding of the nonlinear optical properties of these materials in solution and in the solid state.



Hemiporphyrazines (Hps) were discovered more than 50 years ago,¹ but their photophysical properties remain enigmatic. Despite a relatively large body of computational results,^{2–9} few experimental photophysical studies have been published.^{9–14} This is due, in part, to the poor solubility properties of hemiporphyrazine free base (HpH₂) (Figure 1A) and its ability to bind water molecules to adopt nonplanar conformations with distinct photophysical properties.^{4,11,15} Together with its sensitivity to acid-catalyzed hydrolysis, tendency to form aggregates, and possibility of excited-state tautomerization, these properties make metal-free hemiporphyrazines like HpH₂ very difficult to fully characterize in solution. Despite these challenges, the recent discovery of large two-photon absorption cross sections of metal-free and metallo Hps will invigorate research aimed at characterizing the basic photophysical properties of hemiporphyrazines in the solid state and in solution.¹⁰

In contrast to porphyrins and phthalocyanines, Hps have nonaromatic 20-electron π systems that readily adopt nonplanar conformations.⁴ As a result of symmetry-forbidden S₀ → S₁ transitions,^{4,9} planar Hps in solution exhibit relatively weak absorbance of visible light ($\epsilon_{532\text{nm}} = 16\text{--}2800\text{ M}^{-1}\text{ cm}^{-1}$)^{1,10} but have relatively strong S₀ → S₂ transitions in the far UV ($\epsilon_{350\text{--}390\text{nm}} = 20\,300\text{--}36\,800\text{ M}^{-1}\text{ cm}^{-1}$).^{1,4,9} Interestingly, the metal-free, anhydrous hemiporphyrazine free base (HpH₂) can exhibit multiple emission maxima (430 and 650 nm) upon

photoexcitation at 380 nm. This “dual emission” was previously ascribed to formation of an emissive HpH₂ tautomer having a fully conjugated 20-electron π system with the loss of aromaticity of each pyridine group (Figure 1B).^{6–9} Since free-base hemiporphyrazines have two sets of inequivalent inner nitrogen atoms, three tautomeric forms are theoretically possible (Figure 1A–C). Computational studies suggest that HpH₂ exists exclusively as tautomeric form “A” in the ground state, while emissive tautomers “B” and “C” are proposed to form as a result of excited-state intramolecular proton transfer (ESIPT) from S₂.^{6–9} While light-induced tautomerization reactions are well-known phenomena in porphyrins and phthalocyanines,¹⁶ the possible role of ESIPT in hemiporphyrazine photophysics has remained conjecture for over 15 years.^{6–9} In light of other possible explanations for the multiwavelength emissions from HpH₂, such as the presence of excitons and/or triplet excited states,^{10,17,18} we became interested in the synthesis and characterization of a metallohemiporphyrazine containing a neutral HpH₂ ligand and a d¹⁰ metal ion having a defined oxidation state to serve as a nontautomerizable analog of HpH₂. Such “neutral-ligand” complexes will have two theoretically possible tautomers where the exchangeable protons are located on the peripheral

Received: August 12, 2011

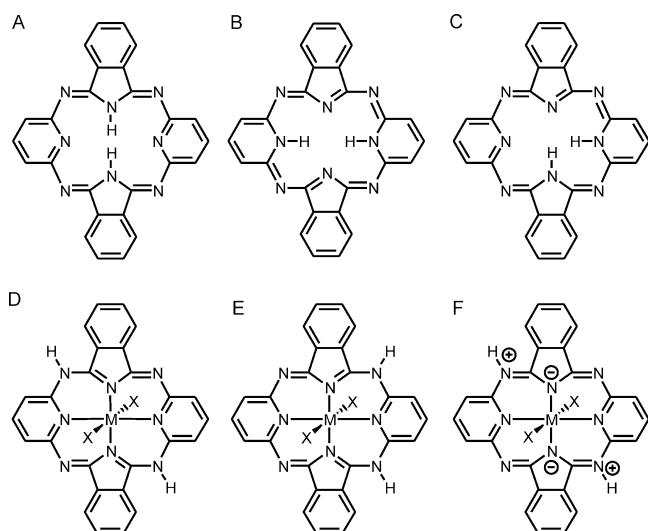
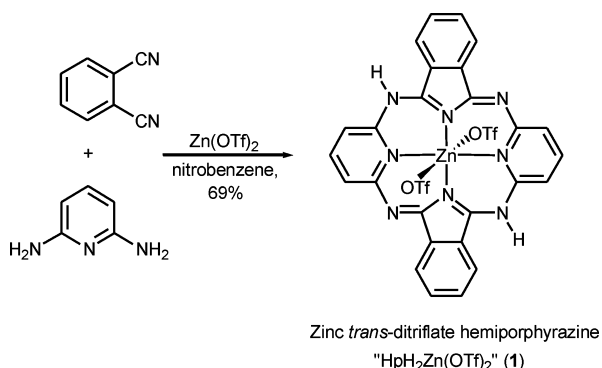


Figure 1. Possible tautomeric forms of HpH_2 (A–C) and $\text{HpH}_2\text{M}(\text{X})_2$ in neutral (D–E) and zwitterionic (F) ligand complexes, where M = divalent metal cation and X = anion.

edge of the macrocycle (Figure 1D and 1E). Given the large distances between the sites of potential exchange, these tautomers will not undergo ESIPT. It was hitherto unknown if these types of metal complexes would exhibit multiple wavelength emission properties similar to HpH_2 and if so what the true basis of this phenomenon might be.

Here we report the synthesis and characterization of an octahedral zinc–hemiporphyrazine “ $\text{HpH}_2\text{Zn}(\text{OTf})_2$ ” (1) (Scheme 1) containing a neutral hemiporphyrazine ligand

Scheme 1. Synthesis of $\text{HpH}_2\text{Zn}(\text{OTf})_2$



that adopts exclusively the C_{2h} -symmetric tautomeric form “D” in the solid state and in solution (Figure 1D). While one can consider a zwitterionic representation of the HpH_2 ligand in this complex (Figure 1F), bond length analyses indicate that the neutral representation (Figure 1D) is more informative. Unlike HpH_2 and $\text{HpH}_2\cdot\text{H}_2\text{O}$, $\text{HpH}_2\text{Zn}(\text{OTf})_2$ is soluble in MeOH, DMSO, and DMF due to the presence of axial ligands on the zinc atom. The improved solubility of this complex allows for concentration-dependent analyses of its photophysical properties. Interestingly, soluble aggregates and solid-state samples of $\text{HpH}_2\text{Zn}(\text{OTf})_2$ exhibit multiple-wavelength photoluminescence properties very similar to those of HpH_2 . For both compounds in the solid state, emissions at 450 nm retain their fluorescence polarization while emissions at 650 nm are depolarized with respect to the excitation source. Taken

together, our results suggest that excitonic coupling of 99 aggregated hemiporphyrazines causes increased absorbance 100 and emission of visible light from $S_0 \leftrightarrow S_1$ transitions that are 101 normally symmetry forbidden in the isolated species.^{4,9} While 102 the participation of emissive triplet states cannot be excluded, 103 we anticipate that the multiwavelength luminescence properties 104 of $\text{HpH}_2\text{Zn}(\text{OTf})_2$ and HpH_2 are a result of emissive $S_2 \rightarrow S_0$ 105 and $S_1 \rightarrow S_0$ transitions. Given the growing interest in 106 hemiporphyrazine-based materials as nonlinear optical devices, 107 these results provide important design considerations 108 by revealing the presence of excitonic luminescence in 109 aggregated and crystalline hemiporphyrazines. 110

MATERIALS AND METHODS

General Methods. Phthalonitrile was purchased from Fluka; all 112 other reagents were obtained in the highest commercially available 113 grades from Sigma Aldrich. ^1H NMR spectra were measured on a 114 Bruker ARX-300 spectrometer (Bruker, Karlsruhe, Germany). The 115 chemical shift values are given in ppm relative to the residual signal 116 from d_6 -DMSO ($\delta = 2.5$ ppm) or MeOD ($\delta = 3.31$ ppm). All data 117 processing was carried out with Topspin (Bruker). Mass spectra were 118 measured at the Institute of Organic Chemistry at the University of 119 Zurich. Electrospray ionization (ESI) mass spectra were measured 120 using an Esquire-LC from Bruker. Absorbance and fluorescence 121 spectra were measured using a Spectra Max M5 from Molecular 122 Devices. 123

Synthesis of $\text{HpH}_2\text{Zn}(\text{OTf})_2$ (1). Phthalonitrile (500 124 mg, 3.90 mmol), 2,6-diaminopyridine (426 mg, 3.90 mmol), and 125 $\text{Zn}(\text{HOTf})_2$ (710 mg, 1.95 mmol) were stirred in nitrobenzene (4 mL) at 220 °C 126 for 4 h under N_2 . The reaction mixture was cooled to room 127 temperature. The resulting precipitate was collected by vacuum 128 filtration, repeatedly washed with CH_2Cl_2 and acetone, and dried in 129 vacuo to yield red crystals (641 mg, 69%). ^1H NMR (300 MHz, 130 MeOD): 8.20 (s br, 2 H), 8.14 (t, $J = 8.0$, 2 H), 7.88–7.82 (m, 8 H), 131 7.51 (d, $J = 8.0$, 4 H). Anal. Calcd for $\text{C}_{28}\text{H}_{16}\text{F}_6\text{N}_8\text{O}_6\text{S}_2\text{Zn}$: C, 41.83; 132 H, 2.01; N, 13.94. Found: C, 41.84; H, 2.18; N, 13.96. 133

Synthesis of Hemiporphyrazine (HpH_2). Phthalonitrile (500 134 mg, 3.90 mmol) and 2,6-diaminopyridine (426 mg, 3.90 mmol) in 1- 135 chloronaphthalene (3 mL) were heated to reflux. After 48 h the 136 solution was cooled to room temperature. The resulting precipitate 137 was isolated by filtration and repeatedly washed with cold methanol. 138 After recrystallization from nitrobenzene, red needles were obtained 139 (1.03 g, 60%). ^1H NMR (300 MHz, d_6 -DMSO): 10.74 (s br, 2 H, 140 NH), 7.99–7.96 (m, 4 H), 7.80–7.76 (m, 6 H); 6.84 (d, $J = 7.8$, 4 H). 141 ESI MS (m/z): $[\text{M} + \text{H}]^+$ calcd for $\text{C}_{26}\text{H}_{17}\text{N}_8$, 441; found, 441. 142

Synthesis of Hemiporphyrazine Monohydrate ($\text{HpH}_2\cdot\text{H}_2\text{O}$). 143 According to published procedures,¹ HpH_2 (50 mg, 0.11 mmol) was 144 stirred in wet benzyl alcohol at 180 °C for 2 h. The reaction mixture 145 was slowly cooled to room temperature over 24 h. The resulting 146 yellow needles were isolated by vacuum filtration and dried in vacuo 147 (51 mg, 98%). 148

X-ray Data Collection and Structure Determination. All 149 measurements were made at 160 K on an Oxford Diffraction 150 SuperNova diffractometer using Mo $K\alpha$ radiation ($\lambda = 0.71073$ Å) 151 for $\text{HpH}_2\text{Zn}(\text{MeOH})_2\cdot 2(\text{OTf})$, Cu $K\alpha$ radiation ($\lambda = 1.54178$ Å) for 152 HpH_2 , and an Oxford Instruments Cryojet XL cooler. Data collection 153 and reduction was performed with CrysAlisPro.²⁰ Intensities were 154 corrected for Lorentz and polarization effects, and an absorption 155 correction based on the multiscan method was applied. Equivalent 156 reflections were merged. Structures were solved by direct methods 157 using SHELXS97.²¹ Least-squares refinement of each structure was 158 carried out on F^2 using SHELXL97 with anisotropic non-hydrogen 159 atoms.²¹ OH and NH hydrogen atoms were placed in the positions 160 indicated by a difference electron density map, and their positions 161 were allowed to refine together with individual isotropic displacement 162 parameters. All remaining H atoms were placed in geometrically 163 calculated positions and refined using a riding model where each H 164 atom was assigned a fixed isotropic displacement parameter with a 165

t1
t2

166 value equal to $1.2U_{eq}$ of its parent C atom ($1.5U_{eq}$ for the methyl
167 groups). Data collection and refinement parameters are given in Table
168 1.

Table 1. Summary of Crystallographic Data

	HpH ₂ Zn(OTf) ₂	HpH ₂
crystallized from	MeOH	1-methylnaphthalene
empirical formula	C ₃₀ H ₂₄ F ₆ N ₈ O ₈ S ₂ Zn	C ₂₆ H ₁₆ N ₈
fw [g/mol]	868.06	440.47
cryst color, habit	red, prism	red, plate
cryst dimens [mm]	0.20 × 0.22 × 0.25	0.05 × 0.11 × 0.20
temp. [K]	160(1)	160(1)
cryst syst	triclinic	monoclinic
space group	$P\bar{1}$	$P2_1/n$
a [Å]	8.2520(2)	14.1690(4)
b [Å]	10.8769(4)	4.9988(1)
c [Å]	11.4996(5)	15.0572(4)
α [deg]	117.121(3)	90
β [deg]	95.376(2)	113.547(3)
γ [deg]	106.102(5)	90
V [Å ³]	852.88(7)	977.66(5)
Z	1	2
ρ _{calcd} [g/cm ³]	1.69	1.496
μ [mm ⁻¹]	0.939	0.764
2θ _(max) [deg]	57	148
total reflns measd	13 290	8403
symmetry independent reflns	3780	1951
R _{int}	0.019	0.072
reflns with I > 2σ(I)	3518	1598
reflns used in refinement	3780	1951
params refined	260	158
final R(F) [I > 2σ(I) reflns]	0.0267	0.0495
wR(F ²) (all data)	0.0703	0.1452
goodness of fit	1.059	1.036
Δρ (max; min) [e Å ⁻³]	0.39; -0.35	0.27; -0.30

169 **Photophysical Measurements.** *Absorbance Measurements in*
170 *Solution.* Solutions of HpH₂Zn(OTf)₂ were prepared at a
171 concentration of approximately 200 μM in dry methanol, and
172 serial dilutions were conducted in a quartz cuvette with a 0.2
173 cm path length over the range of 200 → 25 μM. Below 25 μM,
174 a cuvette with a 1 cm path length was used. All reported
175 absorbance data exhibited raw absorbance values of less than 1
176 AU.

177 *Absorbance Measurements in KBr.* A 0.3 mg amount of each
178 compound was ground with 200 mg of KBr in a mortar and pestle for
179 5 min. The resulting powder was pressed into a pellet under reduced
180 pressure using a Specac 15T manual hydraulic press. The resulting
181 pellets were 13 mm in diameter and 1 mm thick and appeared
182 transparent to the eye. Pellets were immediately measured at an angle
183 of 30° with respect to the incident beam.

184 *Fluorescence Measurements in Solution.* Solutions of HpH₂Zn-
185 (OTf)₂ were prepared at ~200 μM in dry methanol, and serial
186 dilutions were conducted in a quartz cuvette with a 1.0 cm path length.
187 All excitation and emission measurements were recorded at an angle of
188 90° with respect to the incident beam, and all raw data were corrected
189 for inner filter effects of absorbance at each wavelength of excitation
190 “A(λ_{ex})”. Corrected values were obtained by multiplication of the raw
191 intensity values by a correction factor “CF”

$$CF = 2.303A(\lambda_{ex}) / (1 - 10^{-A(\lambda_{ex})}) \quad (1)$$

192 *Fluorescence Measurements in the Solid State.* Crystalline
193 substances were ground into a powder and loaded into a polystyrene
194 96-well plate to a depth of approximately 0.5 mm. All excitation and
195 emission measurements were recorded at an angle of 0° with respect

to the incident beam. Emission and polarization spectra were collected
by exciting the samples at 350 nm and using a long-pass emission filter
at 420 nm. No correction of the raw data was conducted.

RESULTS

199

Synthesis and Structures. Unlike porphyrins and
phthalocyanines, Hps have highly asymmetric coordination
geometries. When coordinated to metals, the two nitrogen
atoms from the isoindole moieties bind more tightly to the
metal while the pyridine units retain much of their original
character.^{22,23} Previous studies have focused on the synthesis of
metallohemiporphyrazines (HpMX_n) where the Hp ligand
carries a -2 or -1 charge in complexes containing Pb(II),¹
Co(II),¹¹ Cu(II),¹¹ V(II),²² Li(I),²⁴ Ni(II),²⁵ Fe(II),²⁶
Mn(II),²⁶ Sn(IV),²⁷ and Cu(II).²⁸ In contrast, there are only a
small number of “neutral-ligand” metallohemiporphyrazines of
the type HpH₂MX₂ reported where M = Cu(II), Ni(II), or
Zn(II) and X = Cl or Br.^{5,11} In these complexes, the charge of
the metal ion is balanced by the axial ligands to give a neutral
HpH₂ ligand. To the best of our knowledge, no crystal structure
or solid-state luminescence properties of such a complex have
previously been reported.

Reactions containing a 2:2:1 mixture of 2,6-diaminopyridine,
phthalonitrile, and Zn(OTf)₂ in refluxing nitrobenzene give a
red crystalline substance HpH₂Zn(OTf)₂ (1) in ~69% isolated
yields (Scheme 1). This new complex is soluble in MeOH,
DMSO, and DMF, and it can be handled in the presence of
oxygen and traces of water without decomposition. Crystals of
HpH₂Zn(OTf)₂ suitable for crystallographic characterization
were grown in solutions of methanol by slow diffusion of
diethyl ether. Two types of crystals were obtained. The first was
a relatively low-quality crystal type which gave a crystal
structure consistent with elemental analysis and NMR data of
HpH₂Zn(OTf)₂ (1). While reliable bond lengths cannot be
ascertained from this X-ray data, the molecular framework and
crystal packing of the model are dependable (Supporting
Information, Figures S1 and S2). In this structure, the Hp
ligand is essentially planar and the axial coordination sites of
octahedral zinc are occupied by triflate ions. The second crystal
type gave very high-quality diffraction data and was found to be
the methanolysis product of HpH₂Zn(OTf)₂ in methanol.
The methanol had displaced the axial triflate ions from zinc, the resulting
structure of HpH₂Zn(MeOH)₂·2(OTf)⁻ is C_{2h} symmetric
(Figure 2), where the two exchangeable N-H protons on the
ligand are at diagonal meso nitrogen atoms. The triflate
counterions (omitted for clarity in Figure 2) act as acceptors of
O-H...O hydrogen bonds from methanol (H...O = 1.95(3) Å
and N-H...O hydrogen bonds from the meso nitrogen atoms
(H...O = 2.13(2) Å). One might consider a zwitterionic
representation for the HpH₂ ligand in this complex (Figure
1F), but bond length analyses indicate the neutral
representation (Figure 1D) is more informative, where the
N1-C1 and N1-C4 bond lengths are highly asymmetric at
1.328(2) and 1.409(2) Å, respectively. Likewise, C1-N4 and
C4-N2 are also asymmetric at 1.331(2) and 1.274(2) Å,
respectively (Figure 2). These bond lengths reveal the presence
of an alternating pattern of single and double bonds consistent
with tautomer “D” (Figure 1D). In contrast, the structure of the
free-base anhydrous ligand HpH₂ (presented below) has nearly
identical N1-C1 and N1-C4 bond distances at 1.392(2) and
1.394(2) Å, respectively, and nearly identical C1-N4 and C4-
N2 bond lengths at 1.282(2) and 1.282(2) Å, respectively
(Figure 3). Notably, the C4-N2 “double” bonds and N1-C4

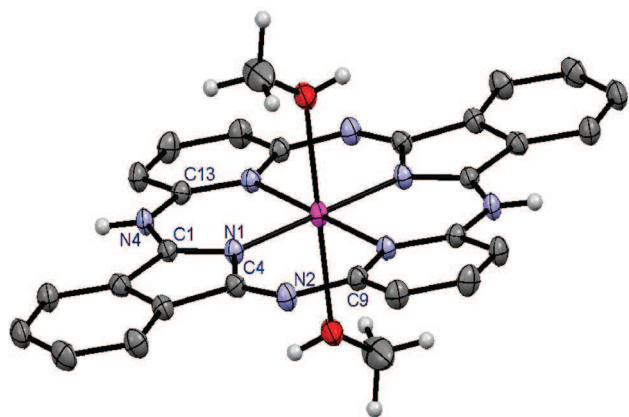


Figure 2. Crystal structure of $\text{HpH}_2\text{Zn}(\text{MeOH})_2 \cdot 2(\text{OTf})$ containing two equivalents of MeOH. Triflate counterions and selected hydrogen atoms have been omitted for clarity; 50% displacement ellipsoids are shown. See the Supporting Information for the lower quality crystal structure of $\text{HpH}_2\text{Zn}(\text{OTf})_2$ (**1**) having axially coordinated triflate ions.

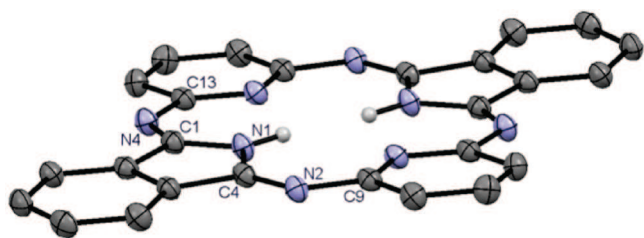


Figure 3. Crystal structure of HpH_2 ; 50% displacement ellipsoids are shown. Selected hydrogen atoms have been omitted for clarity.

3.939(2) and 4.461(2) Å, respectively. Given the small but significant differences in bond lengths in these compounds (discussed in greater detail in the previous paragraph), it was hitherto unknown if HpH_2 and $\text{HpH}_2\text{Zn}(\text{OTf})_2$ would exhibit similar or diverse photophysical properties. To provide a nonplanar hemiporphyrizine for comparison, we also synthesized hemiporphyrizine monohydrate ($\text{HpH}_2 \cdot \text{H}_2\text{O}$),¹ for which a good crystallographic analysis has already been reported (Figure 4, $R = 0.068$).¹⁵ This structure is characterized by a

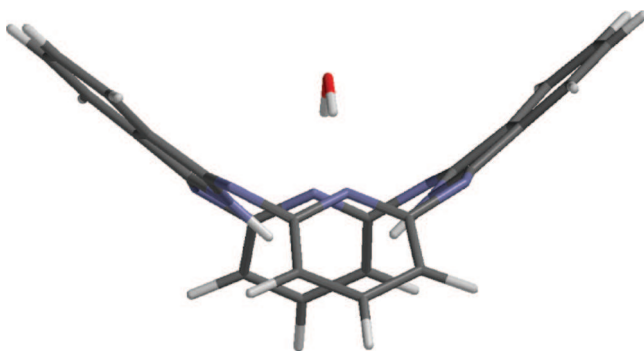


Figure 4. Published crystal structure of $\text{HpH}_2 \cdot \text{H}_2\text{O}$.¹⁵

nonplanar, “saddle”-shape conformation. Interestingly, the N2–C9 bond lengths in $\text{HpH}_2 \cdot \text{H}_2\text{O}$ of 1.411(4) Å are slightly longer than the corresponding N2–C9 bonds of 1.394(2) Å in both HpH_2 and $\text{HpH}_2\text{Zn}(\text{MeOH})_2 \cdot 2(\text{OTf})$. This is consistent with a greater extent of π conjugation across the pyridine units in HpH_2 and $\text{HpH}_2\text{Zn}(\text{MeOH})_2 \cdot 2(\text{OTf})$ as compared to $\text{HpH}_2 \cdot \text{H}_2\text{O}$. This conclusion is supported by trends in the absorbance and fluorescence properties of these compounds.

Photophysical Properties in Solution. Solutions of 56 μM $\text{HpH}_2\text{Zn}(\text{OTf})_2$ (**1**) in MeOH exhibit multiple emissions centered at 430 and 630 nm upon photoexcitation at 380 nm (Figure 5). A similar phenomenon was reported for the

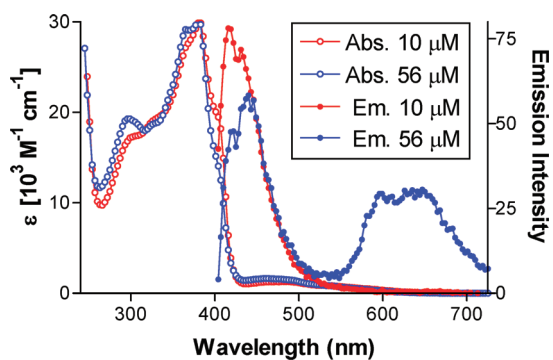


Figure 5. Absorbance (Abs) and emission (Em) spectra of $\text{HpH}_2\text{Zn}(\text{OTf})_2$ at two different concentrations in methanol. Emission spectra were obtained using excitation at 380 nm.

anhydrous, metal-free ligand HpH_2 in DMF.⁷ In our experience and those of others, crystalline HpH_2 is an insoluble material that readily converts into the nonplanar, yellow monohydrate ($\text{HpH}_2 \cdot \text{H}_2\text{O}$) in solvents containing even small traces of H_2O .^{1,11} This has a profound influence on its photophysical properties^{4,9} and furthermore complicates any rigorous analysis of the concentration-dependent luminescence properties of anhydrous HpH_2 in solution. In contrast, $\text{HpH}_2\text{Zn}(\text{OTf})_2$ provides a highly soluble model complex for the neutral

“single” bonds have nearly identical lengths in both HpH_2 and $\text{HpH}_2\text{Zn}(\text{MeOH})_2 \cdot 2(\text{OTf})$. These results are consistent with the neutrality of the Hp ligand in both structures. This conclusion is further supported by the similar photophysical properties exhibited by these materials as well as the lack of acidity exhibited by $\text{HpH}_2\text{Zn}(\text{OTf})_2$ (**1**) in methanol/water mixtures. For all experiments reported here, deprotonation of $\text{HpH}_2\text{Zn}(\text{OTf})_2$ in solution to give an anionic ligand can be excluded, because this reaction is accompanied by a characteristic color change from red to green and the loss of solubility.¹¹ Despite many decades of research, only a single, relatively low-quality crystal structure of the anhydrous hemiporphyrizine ligand (HpH_2) was available, apparently refined without hydrogen atoms ($R = 0.115$).²⁹ HpH_2 was therefore prepared according to modified published procedures,³⁰ and red crystals of HpH_2 suitable for single crystal X-ray diffraction were grown by slow cooling (180–25 °C) of a saturated solution in 1-methylnaphthalene under an inert atmosphere (Figure 3). The resulting structure at 160 K ($R = 0.049$) was found to have different unit cell parameters than the previously published structure.²⁹ Aside from some small distortions similar to those observed in $\text{HpH}_2(\text{MeOH})_2 \cdot 2(\text{OTf})$, HpH_2 adopts a nearly planar structure. Despite the presence of repulsive interactions between the isoindole hydrogen atoms in the center of the macrocycle (N–H···H–N distance = 2.12(3) Å), tautomer “A” of HpH_2 is present in our crystal structure (Figures 1A and 3). The nitrogen atoms of the isoindole moieties are separated by 3.867(2) Å, while the distance between the two pyridyl nitrogen atoms is 4.506(2) Å (Figure 3). These distances are similar to those observed in $\text{HpH}_2\text{Zn}(\text{MeOH})_2 \cdot 2(\text{OTf})$ at

318 HpH_2 ligand to evaluate the potential impact of aggregation on
 319 the photophysical properties of planar HpH_2 .
 320 Serial dilutions of $\text{HpH}_2\text{Zn}(\text{OTf})_2$ conducted at room
 321 temperature in MeOH revealed concentration-dependent
 322 absorbance and fluorescence spectra. With increasing concen-
 323 trations of $\text{HpH}_2\text{Zn}(\text{OTf})_2$, increased molar extinction
 324 coefficients from 430 to 500 nm were observed (Figure 6).

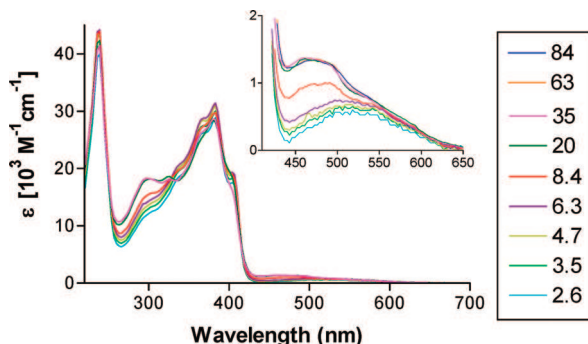


Figure 6. Absorbance spectra of $\text{HpH}_2\text{Zn}(\text{OTf})_2$ as a function of concentration (reported in micromolar) in MeOH.

325 This is the same wavelength range predicted for symmetry-
 326 forbidden $S_0 \rightarrow S_1$ transitions in HpH_2 .^{4,9} Changes in
 327 luminescence also occur with increasing concentrations of
 328 $\text{HpH}_2\text{Zn}(\text{OTf})_2$ in MeOH, where a linear increase in
 329 fluorescence intensity ($\text{Ex} = 380$ nm, $\text{Em} = 450$ nm) was
 330 observed from 0.1 to 5 μM , followed by a decrease in emission
 331 from 7 to 15 μM (Supporting Information, Figure S3). This
 332 type of linear increase of fluorescence followed by self-
 333 quenching is consistent with a monomer–dimer equilibrium
 334 between 0.1 and 15 μM . In contrast, no detectable fluorescence
 335 emission was observed at 600–700 nm over the same
 336 concentration range. At concentrations above 20 μM , however,
 337 a nonsaturating increase in fluorescence emission was observed
 338 at 650 nm, suggestive of aggregate formation (Figure 5 and
 339 Supporting Information, Figure S3). Concentration-dependent
 340 excitation spectra ($\text{Em} = 650$ nm) at concentrations above 20
 341 μM revealed two excitation maxima centered at 350 and 450
 342 nm (Supporting Information, Figure S4). These wavelengths
 343 are similar to those predicted for $S_0 \rightarrow S_2$ and $S_0 \rightarrow S_1$
 344 transitions in HpH_2 .^{4,9}

345 To evaluate the potential role of aggregation in the
 346 concentration-dependent photophysical properties of HpH_2Zn -
 347 $(\text{OTf})_2$, serial dilutions were conducted in DMSO (Supporting
 348 Information, Figure S5). In contrast to the results obtained in
 349 pure methanol (Figure 6), these dilutions obeyed Beer's law
 350 over the entire visible region (Supporting Information, Figure
 351 S5). In addition, no luminescent emissions at 650 nm were
 352 observed from concentrated $\text{HpH}_2\text{Zn}(\text{OTf})_2$ solutions pre-
 353 pared in pure DMSO (Supporting Information, Figure S6). To
 354 further evaluate the solvent-dependent emissions at 650 nm, 83
 355 μM solutions of $\text{HpH}_2\text{Zn}(\text{OTf})_2$ were monitored ($\text{Ex} = 380$
 356 nm) while the solvent composition was varied from 100%
 357 methanol to 100% DMSO. With increasing DMSO concen-
 358 trations, the emissions at 650 nm gradually decreased while the
 359 emissions at 430 nm dramatically increased (Supporting
 360 Information, Figure S6). Taken together, these results suggest
 361 that DMSO is able to inhibit aggregation of $\text{HpH}_2\text{Zn}(\text{OTf})_2$
 362 and that aggregation reactions are indeed responsible for the
 363 concentration-dependent photophysical properties of HpH_2Zn -
 364 $(\text{OTf})_2$ observed in pure methanol (Figures 5 and 6).

Photophysical Properties: Solid State. The limited
 365 solubility of HpH_2 and its tendency to bind water molecules
 366 prevent reliable concentration-dependent characterization of its
 367 photophysical properties in solution.^{1,4,9,11} We therefore
 368 prepared samples in the solid state by grinding each crystalline
 369 substance with KBr and pressing pellets. Both HpH_2 and
 370 $\text{HpH}_2\text{Zn}(\text{OTf})_2$ exhibit relatively strong absorbances between
 371 450 and 600 nm in the solid state with distinct features at 500
 372 and 550 nm (Figure 7). The saddle-shaped compound 373

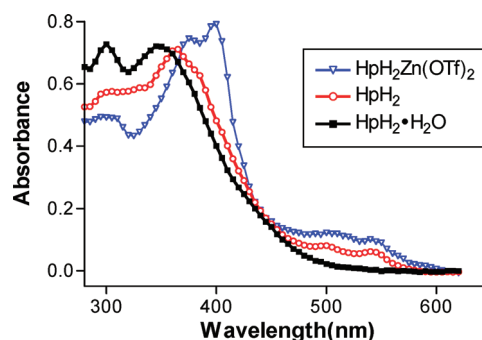


Figure 7. Absorbance spectra of $\text{HpH}_2\text{Zn}(\text{OTf})_2$, HpH_2 , and $\text{HpH}_2\cdot\text{H}_2\text{O}$ prepared in pressed KBr pellets at 0.3 mg/200 mg KBr with an optical path length of 1 mm. See Supporting Information Figure S7 for raw data including KBr blank.

$\text{HpH}_2\cdot\text{H}_2\text{O}$, in contrast, lacks these absorbance features (Figure
 374 7 and Supporting Information, Figure S7).

375 Due to high background emissions and light scattering by
 376 KBr pellets, fluorescence emission data were collected using
 377 thick layers of neat, microcrystalline materials randomly
 378 deposited on polystyrene surfaces. Upon excitation at 350
 379 nm, HpH_2 , $\text{HpH}_2\text{Zn}(\text{OTf})_2$, and $\text{HpH}_2\text{Zn}(\text{MeOH})_2\cdot 2(\text{OTf})_2$
 380 exhibit nearly identical emission spectra, with multiple emission
 381 peaks centered at 450, 480, 650, and 720 nm (Figure 8). 382

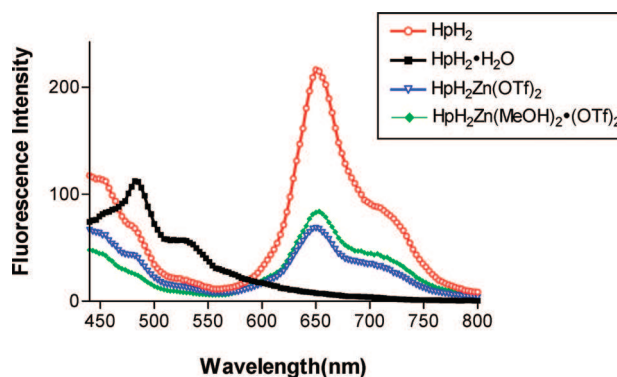


Figure 8. Fluorescence emission spectra of randomly deposited microcrystalline materials using excitation at 350 nm and a long-pass emission filter at 420 nm.

$\text{HpH}_2\cdot\text{H}_2\text{O}$, in contrast, exhibits multiple emission peaks
 383 centered at 450, 480, and 530 nm. Crystal packing effects
 384 have a limited influence on the photophysical properties
 385 reported here. These crystalline materials exhibit highly diverse
 386 packing geometries (Supporting Information, Figures S2 and
 387 S8–S10), but crystals of $\text{HpH}_2\text{Zn}(\text{MeOH})_2\cdot 2(\text{OTf})_2$ and HpH_2
 388 exhibit absorbance, emission, and polarization spectra nearly
 389 identical to $\text{HpH}_2\text{Zn}(\text{OTf})_2$ (1) (Figures 7–9). The relative
 390 emission intensities from crystalline samples of HpH_2 and 391

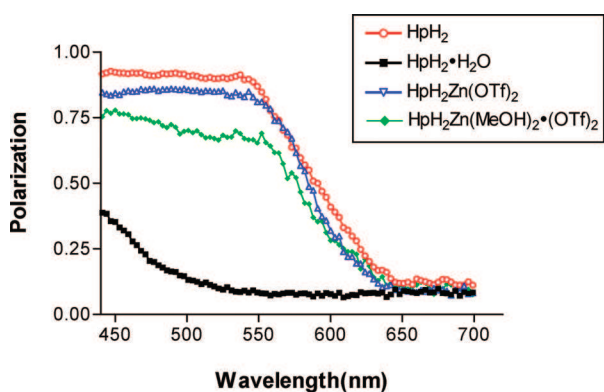


Figure 9. Fluorescence polarization of randomly deposited microcrystalline materials using excitation at 350 nm, an excitation cutoff filter at 420 nm, and plane-polarized excitation and emission with an angle of incidence = 0°. Polarization is calculated as $P = (I_v - I_h)/(I_v + I_h)$, where I_v is the intensity with parallel plane-polarized filters and I_h the intensity with perpendicular plane-polarized filters. These data have not been corrected for instrument response.

392 $\text{HpH}_2\text{Zn}(\text{OTf})_2$ at 650 nm versus 440 nm are somewhat
393 greater for the neat materials (Figure 8) as compared to the
394 soluble aggregates in solution (Figure 5). Together with the
395 concentration-dependent excitation and emission observed in
396 methanol and DMSO (Supporting Information, Figures S3, S4,
397 and S6), these data demonstrate that the emissions at 650 nm
398 are a result of discrete transitions present in aggregated and
399 crystalline hemiporphyrazines.

400 For insight into the nature of multiple-wavelength emissions
401 from HpH_2 and $\text{HpH}_2\text{Zn}(\text{OTf})_2$, fluorescence emission spectra
402 were collected using plane-polarized filters and excitation at 350
403 nm.^{31,32} Neat samples of HpH_2 , $\text{HpH}_2\text{Zn}(\text{OTf})_2$, and
404 $\text{HpH}_2\text{Zn}(\text{MeOH})_2 \cdot 2(\text{OTf})$ exhibit very similar behavior,
405 where emissions from 400 to 550 nm are highly polarized
406 while emissions from 650 to 700 nm are depolarized (Figure
407 9). Soluble aggregates of $\text{HpH}_2\text{Zn}(\text{OTf})_2$ in methanol also give
408 depolarized emissions at 650 nm (Supporting Information,
409 Figure S11). Given the aggregation-dependent nature of these
410 emissions, these polarization data suggest formation of
411 delocalized (excitonic) excited state(s) of these materials that
412 emit depolarized photons between 600 and 700 nm.

413 ■ DISCUSSION

414 Due to its 20-electron, nonaromatic π system, hemiporphyr-
415 azines can readily adopt nonplanar conformations. By
416 modulating the extent of π conjugation, the relative planarity
417 of HpH_2 has a large influence on its photophysical properties.
418 For example, luminescent emissions from $\text{HpH}_2\text{Zn}(\text{OTf})_2$ and
419 HpH_2 in the solid state (650–700 nm) are red shifted by
420 approximately 180 nm as compared to the emissions from the
421 nonplanar monohydrate $\text{HpH}_2 \cdot \text{H}_2\text{O}$ (Figure 8). In addition,
422 $\text{HpH}_2 \cdot \text{H}_2\text{O}$ exhibits relatively little absorbance of visible light in
423 the solid state or in solution (Figure 7 and Supporting
424 Information, Figure S12). The planar Hp ligands present in
425 solid-state samples of $\text{HpH}_2\text{Zn}(\text{OTf})_2$ and HpH_2 , in contrast,
426 exhibit relatively strong absorbance from 450 to 600 nm
427 (Figure 7). These wavelengths are similar to the “Q-band”
428 transitions of 18 π electron porphyrins and phthalocya-
429 nines.^{33–36}

430 The aggregation of $\text{HpH}_2\text{Zn}(\text{OTf})_2$ has a profound impact
431 on its photophysical properties. Upon aggregation in solution,

luminescent emissions at 600–650 nm become apparent while
the emissions at 400–450 nm are diminished (Figure 5 and
Supporting Information, Figure S6). Previous studies have
speculated that the multiple-wavelength emissions from HpH_2
are a result of excited-state intramolecular proton transfer
reactions (ESIPT).^{6–9} However, $\text{HpH}_2\text{Zn}(\text{OTf})_2$ is incapable
of ESIPT and yet exhibits absorbance, multiwavelength
emissions, and polarization spectra very similar to those of
 HpH_2 (Figures 7–9). Our results therefore disprove ESIPT as
the basis of the “dual-emission” properties of these compounds
in the solid state.^{6–9} The exact mechanism for the multiple-
wavelength emissions from aggregated and crystalline hemi-
porphyrazines remains an open question. One possible
explanation is the presence of short-lived triplet states.^{10,17,18}
We were unable, however, to detect any O_2 sensitivity or long-
lived emissions (greater than 10 ns) from soluble aggregates of
 $\text{HpH}_2\text{Zn}(\text{OTf})_2$ in solution. Another explanation is that $\text{S}_2 \rightarrow$
 S_0 (~450 nm) and $\text{S}_1 \rightarrow \text{S}_0$ (~650 nm) transitions are
responsible for multiwavelength emissions from hemiporphyr-
azines. This property is already well known for porphyrins and
phthalocyanines,^{33–36} where aggregation has been shown to
increase the $\text{S}_2 \rightarrow \text{S}_0$ or “Soret” emissions from these aromatic
compounds.^{34,35} Our results, in contrast, suggest a greater
efficiency of $\text{S}_1 \rightarrow \text{S}_0$ emission from aggregated hemi-
porphyrazines. In isolation, $\text{S}_0 \leftrightarrow \text{S}_1$ transitions are normally
symmetry forbidden in hemiporphyrazines,^{4,9} but excitonic
coupling present in aggregated and crystalline hemiporphyr-
azines may increase the oscillator strength of this transition due
to its coupling with $\text{S}_0 \rightarrow \text{S}_2$ transitions. Porphyrins and
phthalocyanines have also been shown to undergo redistrib-
ution of transition dipole strengths between their “B bands”
(~400 nm) and “Q bands” (500–650 nm) upon aggregation in
solution due to excitonic coupling between these transition
dipoles.³¹ Similar effects may be present for $\text{HpH}_2\text{Zn}(\text{OTf})_2$,
where dilute solutions exhibit strong absorbance centered at
370 nm and little, if any, absorbance at 450 nm, and aggregated
samples exhibit increased extinction coefficients at 300 and 450
nm and decreased extinction coefficients from 330 to 400 nm
(Figure 6). Interestingly, these changes are accompanied by the
emergence of isotropic fluorescent emissions at 650–700 nm
(Figures 6 and 8). Taken together, these results suggest the
presence of enhanced $\text{S}_0 \leftrightarrow \text{S}_1$ transitions in aggregated
hemiporphyrazines due to the presence of excitonic coupling
with $\text{S}_0 \leftrightarrow \text{S}_2$ transitions.^{4,9} Given the growing interest in
hemiporphyrazine-based materials as nonlinear optical devi-
ces,^{17,19} these results provide important new design consid-
erations by highlighting the differences in photophysical
properties of planar versus nonplanar hemiporphyrazines as
well as the presence of excitonic luminescence from aggregated
and crystalline hemiporphyrazines.

■ ASSOCIATED CONTENT

Supporting Information

X-ray crystallographic data of $\text{HpH}_2\text{Zn}(\text{MeOH})_2 \cdot 2(\text{OTf})$ and
 HpH_2 in CIF format; preliminary X-ray structure of $\text{HpH}_2\text{Zn}-$
 $(\text{OTf})_2$; crystal packing diagrams and solvent-dependent
absorption and emission spectra. This material is available
free of charge via the Internet at <http://pubs.acs.org>.

■ AUTHOR INFORMATION

Corresponding Author

*Phone: +41 44 635 4244. Fax: +41 44 635 6891. E-mail:
luedtke@oci.uzh.ch.

Notes

The authors declare no competing financial interest.

ACKNOWLEDGMENTS

This work was supported by the University of Zürich and the Swiss National Science Foundation #130074.

REFERENCES

- (1) Elvidge, J. A.; Linstead, R. P. *J. Chem. Soc.* **1952**, 5008–5012.
- (2) Bossa, M.; Cervone, E.; Garzillo, C.; Del Re, G. *J. Mol. Struct. (THEOCHEM)* **1995**, 342, 73–86.
- (3) Honeybourne, C. L. *J. Chem. Soc., Chem. Commun.* **1972**, 213–214.
- (4) Zakharov, A. V.; Stryapan, M. G.; Islyaikin, M. K. *J. Mol. Struct. (THEOCHEM)* **2009**, 906, 56–62.
- (5) Bossa, M.; Grella, I.; Nota, P.; Cervone, E. *J. Mol. Struct. (THEOCHEM)* **1990**, 210, 267–271.
- (6) Peluso, A.; Garzillo, C.; Del Re, G. *Chem. Phys.* **1996**, 204, 347–351.
- (7) Altucci, C.; Borrelli, R.; de Lisio, C.; De Riccardis, F.; Persico, A.; Porzio, A.; Peluso, A. *Chem. Phys. Lett.* **2002**, 354, 160–164.
- (8) Persico, V.; Carotenuto, M.; Peluso, A. *J. Phys. Chem. A* **2004**, 108, 3926–3931.
- (9) Bossa, M.; Cervone, E.; Garzillo, C.; Peluso, A. *J. Mol. Struct. (THEOCHEM)* **1997**, 390, 101–107.
- (10) Dini, D.; Calvete, M. J. F.; Hanack, M.; Amendola, V.; Meneghetti, M. *J. Am. Chem. Soc.* **2008**, 130, 12290–12298.
- (11) Attanasio, D.; Collamati, I.; Cervone, E. *Inorg. Chem.* **1983**, 22, 3281–3287.
- (12) Dirk, C. W.; Marks, T. J. *Inorg. Chem.* **1984**, 23, 4325–4332.
- (13) Anderson, J. S.; Bradbrook, E. F.; Cook, A. H.; Linstead, R. P. *J. Chem. Soc.* **1938**, 1151–1156.
- (14) Birch, C. G.; Iwamoto, R. T. *Inorg. Chem.* **1973**, 12, 66–73.
- (15) Peng, S.-M.; Wang, Y.; Ho, T.-F.; Chang, I.-C.; Tang, C.-P.; Wang, C.-J. *J. Chin. Chem. Soc.* **1986**, 33, 13–21.
- (16) Chizhika, A. M.; Jäger, R.; Chizhika, A. I.; Bära, S.; Macka, H.-G.; Sackrowa, M.; Stanciu, C.; Lyubimtseva, A.; Hanack, M.; Meixner, A. *J. Phys. Chem. Chem. Phys.* **2011**, 13, 1722–1733.
- (17) Dini, D.; Calvete, M. J. F.; Hanack, M.; Amendola, V.; Meneghetti, M. *Chem. Commun.* **2006**, 2394–2396.
- (18) Möllerstedt, H.; Crespo, R.; Piqueras, C.; Ottosson, H. *J. Am. Chem. Soc.* **2004**, 126, 13938–13939.
- (19) De la Torre, G.; Gray, D.; Blau, W.; Torres, T. *Synth. Met.* **2001**, 121, 1481–1482.
- (20) *CrysAlisPro*; Oxford Diffraction Ltd.: Yarnton, Oxfordshire, England, 2010.
- (21) Sheldrick, G. M. *Acta Crystallogr., Sect. A* **2008**, 64, 112–122.
- (22) Esposito, J. N.; Sutton, L. E.; Kenney, M. E. *Inorg. Chem.* **1967**, 6, 1116–1120.
- (23) Sutton, L. E.; Kenney, M. E. *Inorg. Chem.* **1967**, 6, 1869–1872.
- (24) Sripothongnak, S.; Pischera, A. M.; Espe, M. P.; Durfee, W. S.; Ziegler, C. J. *Inorg. Chem.* **2009**, 48, 1293–1300.
- (25) Agostinelli, E.; Attanasio, D.; Collamati, I.; Fares, V. *Inorg. Chem.* **1984**, 23, 1162–1165.
- (26) Collamati, I.; Cervone, E.; Scoccia, R. *Inorg. Chim. Acta* **1985**, 98, 11–17.
- (27) Farris, P. J.; Jacobs, J. T.; Okonczac, M. P.; Durfee, W. S.; Noll, B. C. *Acta Crystallogr.* **1999**, C55, 32–33.
- (28) Matassa, R.; Cervone, E.; Sadun, C. *J. Porphyrins Phthalocyanines* **2003**, 7, 579–584.
- (29) Peng, S.-M.; Wang, Y.; Chen, C. K.; Lee, J. Y.; Liaw, D. S. *J. Chin. Chem. Soc.* **1986**, 33, 23–33.
- (30) Honeybourne, C. L.; Burchill, P. *Inorg. Synth.* **1978**, 18, 44–49.
- (31) Zimmermann, J.; Siggel, U.; Fuhrhop, J.-H.; Röder, B. *J. Phys. Chem. B* **2003**, 107, 6019–6021.
- (32) Sissa, C.; Painelli, A.; Blanchard-Desce, M.; Terenziani, F. *J. Phys. Chem. B* **2011**, 115, 7009–7020.
- (33) Kobayashi, N.; Lever, A. B. P. *J. Am. Chem. Soc.* **1987**, 109, 5587433–7441.
- (34) Pérez-Morales, M.; de Miguel, G.; Bolink, H. J.; Martín-Romero, M. T.; Camacho, L. *J. Mater. Chem.* **2009**, 19, 4255–4260.
- (35) Fujitsuka, M.; Won Cho, D.; Solladié, N.; Troiani, V.; Qiu, H.; Majima, T. *J. Photochem. Photobiol. A* **2007**, 188, 346–350.
- (36) Akimoto, S.; Yamazaki, T.; Yamazaki, I.; Osuka, A. *Chem. Phys. Lett.* **1999**, 309, 177–182.